 SDHM, vol.5, no.3, pp.201-226, 2009

Residual Strength Evaluation of Unstiffened and Stiffened Panels under Fatigue Loading

A. Rama Chandra Murthy[1], **G.S. Palani**[1] **and Nagesh R. Iyer**[1]

Abstract: This paper presents methodologies for residual strength evaluation of metallic structural components under fatigue loading. Structural components include plate panels of different crack configurations with and without stiffeners. For stiffened panels, stress intensity factor (SIF) has been computed by using parametric equations based on numerically integrated modified virtual crack closure integral (NI-MVCCI) technique. As a part of residual strength evaluation, remaining life has also been predicted by using standard crack growth models. Various methodologies for residual strength evaluation, namely, plastic collapse condition, fracture toughness criterion and remaining life approach have been described. From the studies, it has been observed that the predicted residual strength using remaining life approach is lower compared to those predicted by using other two approaches and will govern the design. In the case of stiffened panels, residual strength has been predicted by using remaining life approach and it is observed that the residual strength increases with the increase of stiffener size. Expressions for residual strength have been proposed considering various stiffener sizes, stiffener position and type of stiffener, which will be useful for designers to design the structural components/structures against fatigue and fracture.

Keywords: Plate panels, Stiffened panels, Stress intensity factor, Fatigue, Fracture, Remaining life, Residual strength

1 Introduction

Reliability and functionality are two of the most important requirements of engineered structures and components. Most of the structures such as nuclear containments, reactor vessels, flyovers, high-rise buildings, aerospace structures, ship hulls, bridges and offshore structures are required to operate under controllable operating conditions. The environment may also be variable, regardless of the operat-

[1] Scientist, Structural Engineering Research centre, CSIR, CSIR Campus, Taramani, Chennai – 600 113, India, email: murthyarc@sercm.org, pal@sercm.org, nriyer@sercm.org.

ing regime. Stiffeners or stringers are mainly provided to improve the strength and stability of the structures and to provide a means of slowing down or arresting the growth of cracks in the panel. Most of the above structures are generally subjected to fatigue loading. The fatigue loading may be either constant amplitude loading or variable amplitude loading. Remaining life or residual strength assessment of the cracked structural components in these structures will be helpful for their in-service inspection, planning, repair, retrofitting, rehabilitation, requalification and health monitoring. Further, it is essential to use the damage tolerant design concepts for designing some of the above structural components. A structural component is damage tolerant if it can sustain cracks of critical length safely until it is repaired or its economic service life has expired. Damage tolerant analysis provides information about the effect of cracks on the strength of the component/structure. This information is usually presented in the form of two diagrams, namely, the residual strength diagram and the crack growth diagram. Fracture mechanics is a tool employed for investigation of the crack growth and fracture behaviour of structural components that are subjected to fatigue loading.

In general, it is difficult to quantify SIF for most of the practical applications. For these applications, SIF is generally calculated based on the procedures and simplified equations presented in handbooks [Rooke and Cartwright (1976); Murakami (1988)]. However, these procedures/equations are applicable only for simple and standard structural components. During the last four decades, a great deal of research has been dedicated to the development of numerical/analytical methods for computation of SIF for stiffened and unstiffened plate panels subjected to uniaxial tensile stresses. Toor (1973) conducted an extensive review on damage tolerant design approaches for aircraft structures. It was pointed out that the residual strength analysis methodology, various crack propagation laws and fracture mechanics can be applied to evaluate damage tolerance capacity of built-up structural components under spectrum loading conditions. The results of the test and finite element analysis (FEA) of complex structures indicated that simple methods of fracture mechanics can be applied to find the degree of damage tolerance. Wood and Howard (1975) discussed the significant factors leading to the development of damage tolerance criteria and illustrated the role of fracture mechanics in the analysis and testing aspects necessary to satisfy these requirements. Swift (1984) conducted fracture analysis of cracked stiffened structure based on displacement compatibility method. Residual strength was computed for a two bay skin crack with a broken stiffener condition. Brussat et al. (1986) presented the details of damage tolerance assessment of aircraft attachment lugs. Toor et al. (1987) explained the details of damage tolerant design of fuselage structures with longitudinal cracks and circumferential cracks. Wen et al. (2002) and Aliabadi et al. (2002) presented bound-

ary element method for damage tolerant assessment of cracked panels. Cali and Citarella (2004) presented a numerical procedure for residual strength assessment of a cracked butt-joint, based on R-curve analysis and plastic collapse prediction. LEFM principles were employed for assessment of residual strength. Wang et al. (2006) presented a numerical method to predict the residual strength of a composite fuselage panel with discrete source damage. Crack growth resistance curve (R-curve) method was used to predict the residual strength. Nathan et al. (2006) predicted residual strength of structural composites subjected to variable amplitude fatigue loading and environmental exposure. Experiments were also carried out on E-glass fibers and vinyl ester resin. Nathan et al. (2008) proposed a simple model for residual strength prediction of composite material under constant amplitude loading and block spectrum loading.

From the literature, it has been observed that residual strength is generally evaluated using plastic collapse condition (net section collapse condition) or fracture toughness criterion. In the present investigation, another method based on remaining life approach is proposed to evaluate the residual strength. Further, it has also been observed that there is a need to evolve efficient methodologies for computation of SIF in the case of stiffened panels and to provide an integrated approach that would include fatigue crack growth models for remaining life and residual strength prediction.

This paper presents methodologies for residual strength evaluation of metallic structural components under fatigue loading. Structural components include plate panels of different crack configurations with and without stiffeners. For stiffened panels, stress intensity factor (SIF) has been computed by using parametric equations developed by using numerically integrated modified virtual crack closure integral (NI-MVCCI) technique. As a part of residual strength evaluation, remaining life has also been predicted by using standard crack growth models. Various methodologies for residual strength evaluation, namely, plastic collapse condition, fracture toughness criterion and remaining life approach have been described. From the studies, it has been observed that the predicted residual strength using remaining life approach is lower compared to those predicted by using other two approaches and will govern the design. In the case of stiffened panels, residual strength has been predicted by using remaining life approach and it is observed that the residual strength increases with the increase of stiffener size. It is further observed that in the case of stiffener at edges the rate of decrease in residual strength w. r. to crack length is uniform for all stiffener sizes, whereas for the case of intermediate stiffener, the rate varies gradually for different stiffener sizes. Expressions for residual strength have been proposed considering various stiffener sizes, stiffener position and type of stiffener, which will be useful for designers to design the structural

components/structures against fatigue and fracture.

2 Computation of SIF

Prediction of the remaining life or residual strength of a fatigue-damaged structural component depends on proper understanding of the crack growth behaviour, which in turn relies on the computation of SIF accurately. SIF of structures/structural components can be computed by using LEFM principles. Irwin (1957) used the classical theory of elasticity to show that the stresses in the vicinity of the crack tip are of the form (Fig. 1)

$$\sigma_{ij} \propto \frac{1}{\sqrt{2\pi r}} f_{ij}(\theta) + \cdots \tag{1}$$

where, r and θ form a polar co-ordinate system with their origin at the crack tip, as shown in Fig. 1, and f_{ij} is a function of θ. The above equation can be written as

$$\sigma_{ij} = \frac{K}{\sqrt{2\pi r}} f_{ij}(\theta) + \cdots \tag{2}$$

where,

$$K = Y\sigma\sqrt{\pi a}. \tag{3}$$

where, Y is a geometric correction factor and σ is the stress to which the crack plane is subjected. The determination of SIF in complex geometries such as cracked stiffened plates is extremely difficult owing to the complexities introduced by the structural geometry and the nature of stress field at the crack tip.

2.1 SIF Computation for stiffened panels

Extensive work on fracture analysis of structural components has been carried out by using the finite element method (FEM) [Palani (2004)]. It is observed from the studies conducted on the fracture analysis of plates that the performance of 9-noded Lagrangian element with assumed shear strain fields exhibit better performance among the other quadrilateral plate elements considered [Palani et al. (2005)]. This element has been appropriately combined with 3-noded beam element for formulating MQL9S2 stiffened plate finite element (FE) model [Palani et al. (2005)]. For tensile mode I and bending mode 1 fracture of stiffened panels, G_I and G_1 can be evaluated by multiplying the stress/moment distribution ahead of crack tip with the corresponding displacement/rotation distribution behind crack tip and integrating this product over Δa (virtual increment of crack length). It may be noted that tensile mode I and bending mode 1 fracture are coupled for plates with eccentric

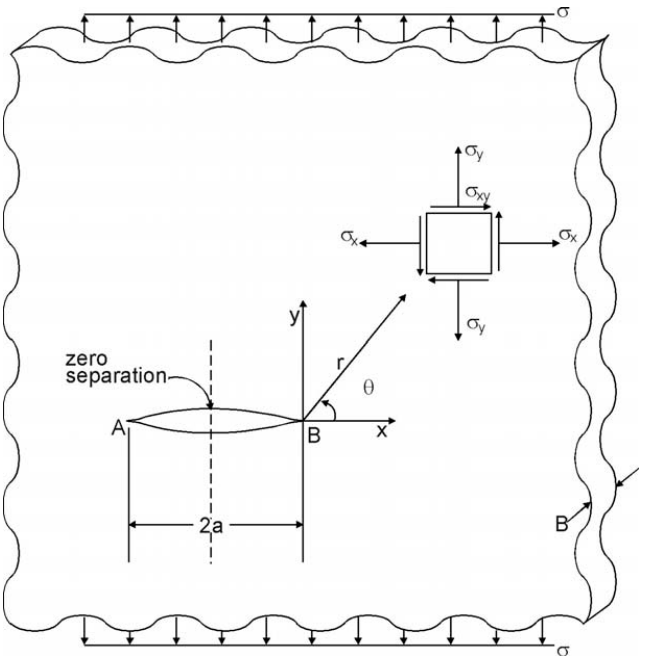

Figure 1: Crack tip co-ordinate system

stiffeners (Refer Fig.2) (G_I and G_1), in view of the transformation matrices related to MQL9S2 FE model. The stress/moment distribution on the crack extension and the crack opening displacement/rotation distribution should be evaluated after duly accounting for the stiffener elements in the respective plate finite elements. Let these be represented as σ_{yyp}, σ_{xyp}, M_{yyp}, M_{xyp} and Q_{zp} and U_{xp}, U_{yp}, U_{zp}, θ_{xp} and θ_{yp}. The subscript 'p' indicates that stress/moment and displacement components are for that of a stiffened plate panel evaluated at the plate mid-surface level. The components of strain energy release rate can then be evaluated based on Irwin's theory using the force and displacement components, which can be expressed as

$$G_I = \lim_{\Delta a \to 0} \frac{1}{2\Delta a} \int_{\Delta a} \sigma_{yyp}(\xi) u_{yp}(\xi') dx \tag{4a}$$

$$G_1 = \lim_{\Delta a \to 0} \frac{1}{2\Delta a} \int_{\Delta a} M_{yyp}(\xi) \theta_y p(\xi') dx \tag{4b}$$

$$G_{II} = \lim_{\Delta a \to 0} \frac{1}{2\Delta a} \int_{\Delta a} \sigma_{xyp}(\xi) u_{xp}(\xi') dx \tag{4c}$$

$$G_2 = \lim_{\Delta a \to 0} \frac{1}{2\Delta a} \int_{\Delta a} Q_{zp}(\xi) w_p(\xi') dx \tag{4d}$$

$$G_3 = \lim_{\Delta a \to 0} \frac{1}{2\Delta a} \int_{\Delta a} M_{xyp}(\xi) \theta_{xp}(\xi') dx \tag{4e}$$

where ε and ε' are the natural coordinate system used to represent the deformations behind the crack tip and the force ahead of the crack tip, respectively. x is the cartesian coordinates along the line ahead of crack tip.

The integrals given in eqn (4) can be obtained by numerical integration technique. The integrals associated with the evaluation of the constants related to the stress/moment distribution and the above integrals are obtained out by using Gauss numerical integration technique with an order of 3 applicable for 9-noded element with assumed transverse shear strain fields [Palani et al. (2005)]. Fig. 2 shows a plate with an eccentric stiffener. If e_x=0.0, the plate will become a case with concentric stiffener.

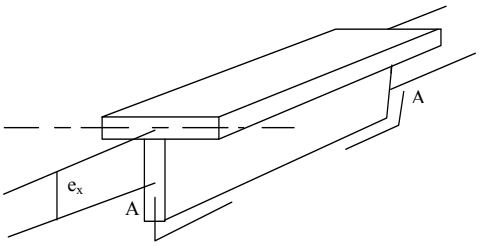

Figure 2: Plate with an eccentric stiffener

Fracture analysis of cracked stiffened plates under combined tensile, bending and shear loads has been conducted by employing MQL9S2 FE model. Parametric studies on fracture analysis of stiffened plates subjected to tension-moment loads have been conducted by employing NI-MVCCI technique and MQL9S2 FE model. Based on the parametric studies, the following equations have been proposed for computation of SIF values of typical stiffened plates subjected to tensile-moment loads [Palani (2005)].

Case a: Tensile loading – Concentric stiffeners

For x_s= 2

$$\beta_I = -73.501\alpha_a^5 + 118.377\alpha_a^4 - 73.068\alpha_a^3 + 22.436\alpha_a^2 - 4.125\alpha_a + 0.581 \tag{5a}$$

For $x_s = 25$

$$\beta_I = -1.586\alpha_a^3 + 2.510\alpha_a^2 - 1.827\alpha_a + 0.631 \tag{5b}$$

For $x_s = 50$

$$\beta_I = -0.8629\alpha_a^3 + 1.6822\alpha_a^2 - 1.5563\alpha_a + 0.6332 \tag{5c}$$

For $x_s = 100$

$$\beta_I = -0.4843\alpha_a^3 + 0.9982\alpha_a^2 - 1.0924\alpha_a + 0.6348 \tag{5d}$$

For $x_s = 150$

$$\beta_I = -0.3307\alpha_a^3 + 0.6351\alpha_a^2 - 0.6521\alpha_a + 0.6349 \tag{5e}$$

For $x_s = 200$

$$\beta_I = -0.1283\alpha_a^3 + 0.2714\alpha_a^2 - 0.3234\alpha_a + 0.6352 \tag{5f}$$

Case b: Tensile loading – Eccentric stiffeners

For $x_s = 25$

$$\beta_1 = 89.65\alpha_i^7 - 303.8\alpha_i^6 + 412.8\alpha_i^5 - 287.67\alpha_i^4 + 109.04\alpha_i^3 - 21.95\alpha_i^2 + 2.03\alpha_i + 0.633 \tag{6a}$$

For $x_s = 50$

$$\beta_1 = 82.65\alpha_i^7 - 280.4\alpha_i^6 + 382.12\alpha_i^5 - 267.48\alpha_i^4 + 101.93\alpha_i^3 - 20.61\alpha_i^2 + 1.92\alpha_i + 0.621 \tag{6b}$$

For $x_s = 100$

$$\beta_1 = 61.75\alpha_i^7 - 208.87\alpha_i^6 + 284\alpha_i^5 - 198.5\alpha_i^4 + 75.58\alpha_i^3 - 15.29\alpha_i^2 + 1.43\alpha_i + 0.63 \tag{6c}$$

For x_s= 150

$$\beta_1 = 36.899\alpha_i^7 - 125.68\alpha_i^6 + 171.99\alpha_i^5 - 120.87\alpha_i^4 + 46.22\alpha_i^3 - 9.37\alpha_i^2 + 0.88\alpha_i + 0.63 \quad (6d)$$

For x_s = 200

$$\beta_1 = 19.02\alpha_i^7 - 64.69\alpha_i^6 + 88.471\alpha_i^5 - 62.17\alpha_i^4 + 23.78\alpha_i^3 - 4.83\alpha_i^2 + 0.454\alpha_i + 0.634 \quad (6e)$$

Case c : Moment loading – Concentric stiffeners

For x_s = 2

$$\beta_1 = 1.4699\alpha_a^4 - 3.1712\alpha_a^3 + 2.5486\alpha_a^2 - 1.0647\alpha_a + 0.25587 \quad (7a)$$

For x_s= 25

$$\beta_1 = -0.4335\alpha_a^3 + 0.9064\alpha_a^2 - 0.8143\alpha_a + 0.3178 \quad (7b)$$

For x_s = 50

$$\beta_1 = -0.3566\alpha_a^3 + 0.7739\alpha_a^2 - 0.7672\alpha_a + 0.3231 \quad (7c)$$

For x_s = 100

$$\beta_1 = -0.3\alpha_a^3 + 0.6667\alpha_a^2 - 0.7285\alpha_a + 0.3247 \quad (7d)$$

For x_s= 150

$$\beta_1 = -0.2297\alpha_a^3 + 0.5666\alpha_a^2 - 0.6819\alpha_a + 0.3245 \quad (7e)$$

For x_s= 200

$$\beta_1 = -0.1233\alpha_a^3 + 0.4130\alpha_a^2 - 0.5895\alpha_a + 0.3230 \quad (7f)$$

Case d: Moment loading – Eccentric stiffeners

For x_s = 5

$$\beta_1 = -24.9994\alpha_i^5 + 73.06\alpha_i^4 - 80.99\alpha_i^3 + 42.515\alpha_i^2 - 11.3838\alpha_i + 1.806 \quad (8a)$$

For x_s = 25

$$\beta_1 = -19.2985\alpha_i^5 + 62.7769\alpha_i^4 - 76.182\alpha_i^3 + 43.109\alpha_i^2 - 12.263\alpha_i + 1.9974 \quad (8b)$$

For x_s = 50

$$\beta_1 = -8.3121\alpha_i^5 + 39.3335\alpha_i^4 - 59.1464\alpha_i^3 + 38.3899\alpha_i^2 - 11.977\alpha_i + 2.0276 \quad (8c)$$

For x_s = 100

$$\beta_1 = 22.3863\alpha_i^4 - 47.701\alpha_i^3 + 35.6974\alpha_i^2 - 12.0033\alpha_i + 2.0484 \quad (8d)$$

For x_s = 150

$$\beta_1 = -11.1204\alpha_i^5 + 45.1797\alpha_i^4 - 63.1028\alpha_i^3 + 39.373\alpha_i^2 - 12.1543\alpha_i + 2.0856 \quad (8e)$$

For x_s = 200

$$\beta_1 = -29.5998\alpha_i^5 + 83.1355\alpha_i^4 - 88.594\alpha_i^3 + 45.0239\alpha_i^2 - 11.9976\alpha_i + 2.1393 \quad (8f)$$

Eqns (5) to (8) are obtained by curve fitting with an accuracy of less than 0.1% error.

where, $\alpha_a = \frac{A_s}{A_p + A_s}$ and $\alpha_i = \frac{I_s}{I_p + I_s}$, x_s = Distance of stiffener from crack tip in mm

where, A_s = Area of stiffener, A_p = Area of plate, I_s = Moment of inertia of stiffener and I_p = Moment of inertia of plate, β_1 = Geometric correction factor.

3 Remaining Life Prediction

The proposed methodology uses LEFM concepts for remaining life prediction. In LEFM, an elastic stress field is defined at crack tip and is characterized in terms of SIF or K alone. The rate of crack growth, da/dN, in terms of the crack tip SIF range, ΔK can be expressed as

$$\frac{da}{dN} = f(\Delta K) \quad (9)$$

Paris, Walker, Forman, Erdogan and Ratwani, Klesnil and Lucas, Forman-Newman-de Koning have contributed with different models representing crack growth behaviour.

The number of loading cycles required to extend the crack from an initial length a_0 to the final critical crack length a_f is given by

$$N = \int_{a0}^{af} \frac{da}{f(\Delta K)} \tag{10}$$

4 Residual Strength Evaluation of Structural Components

Damage tolerance analysis provides capability for the calculation of both residual strength diagram (fracture due to cracks) and crack growth curve. Procedure for prediction of remaining life is described above. Residual strength can be computed by using

(i) plastic collapse condition or yield criterion

(ii) Fracture toughness criterion and

(iii) Remaining life approach

The residual strength of a plate/panel is the least value obtained by using the above three criterions.

In general, construction of a residual strength diagram involves three major steps:

(a) Development of the relationship between the applied stress σ, the crack length parameter 'a', and the applied SIF, 'K' for the given structural configuration.

(b) Selection of an appropriate failure criterion based on the expected material behavior at the crack tip

(c) The fracture strength (σ_{fc}) values for critical crack sizes (a_c) are obtained by utilizing the results of the first two steps. The residual strength diagram (σ_f vs. a_c) for the given structural configuration is plotted based on these values.

(i) Plastic collapse condition

In the plane stress condition, where the stress in the entire cross section is equal to yield strength at the time of collapse, the maximum load carrying (P_{max}) capacity of the plate with an edge crack is [David Broek (1989)]

$$P_{max} = t(W - a)\sigma_y \tag{11}$$

where, a = crack length, W = total width, t = thickness, and σ_y = yield strength.

This failure load is called the collapse load or the limit load.

The nominal stress in full width of the component is,

$$\sigma_{=}\frac{P_{\max}}{Wt} \tag{12}$$

Hence the component fails when the nominal stress is,

$$\sigma_{fc} = \frac{P_{\max}}{Wt} = \frac{t(W-a)\sigma_y}{Wt} \tag{13}$$

If a = W, failure will occur when the nominal stress $\sigma_{fc} = 0$

(ii) Fracture toughness criterion

The nominal stress at which fracture takes place, will be denoted as σ_{fc} (Palani[14]).

$$\sigma_{fc} = \frac{\text{Fracture toughness}}{\beta\sqrt{\pi a}} \tag{14}$$

where, σ_{fc} is the residual strength or the remaining strength under the presence of cracks.

(iii) Remaining life approach

Irwin proposed the following SIF K_s to quantify the intensity of the stress field surrounding the crack tip in a finite width plate with a remote stress, σ:

$$K_s = \beta\sigma\sqrt{\pi a} \tag{15}$$

where a = half-length of the crack, β = Geometry factor

Hence such a plate with a half crack a_x will fracture when the applied stress σ_x satisfies the equation

$$K_c = \beta\sigma_x\sqrt{\pi a_x} \tag{16}$$

where K_c= critical SIF, which is a material property. The rate at which the crack grows under constant amplitude cyclic loading can be derived from the following equation that was proposed by [Paris (1963)].

$$da/dN = C(\Delta K)^m \tag{17}$$

which can be written in the following integral form to give the number of cycles N_f that are required for a crack of initial length a_i to propagate to a crack length a_x:

$$N_f = \int_{a_i}^{a_x} \frac{da}{C(\Delta K)^m} \tag{18}$$

where C and m are Crack growth constants and ΔK= range of SIF corresponding to the cyclic load $\Delta\sigma$.

From eqn.(15)

$$\Delta K = \beta \Delta\sigma \sqrt{\pi a} \tag{19}$$

and from eqn. (16)

$$a_x = K_c^2 / \beta^2 \sigma_x^2 \pi \tag{20}$$

Substituting eqns.(19) and (20) into eqn.(17) and integrating gives the following residual strength curve, where σ_c is the residual strength after N_c cycles of load:

$$N_c = D_1 - S_1 (1/\sigma_c^2)^{(1-(m/2))} \tag{21}$$

where

$$D_1 = (a_i)^{1-(m/2)} / \left[C\beta^m (\Delta\sigma)^m \pi^{\frac{m}{2}} \left(\frac{m}{2} - 1 \right) \right] \tag{22}$$

and

$$S_1 = \left(\frac{K_c^2}{\beta^2 \pi} \right)^{1-(m/2)} / \left[C\beta^m (\Delta\sigma)^m \pi^{\frac{m}{2}} \left(\frac{m}{2} - 1 \right) \right] \tag{23}$$

where for a fixed initial crack size a_i, the parameters D_1 and S_1 are constants.

5 Numerical Studies

To demonstrate the methodologies described in the paper, studies have been conducted for remaining life prediction and residual strength assessment. Three example problems, namely, (i) plate with a centre crack made up of 350 WT Steel (ii) Compact tension specimen made up of 2024-T3 Al alloy and (iii) Stiffened plate with centre crack made up of 2024-T3 Al alloy subjected to constant amplitude loading have been presented herein.

5.1 Plate with centre crack - 350WT Steel

This example was studied by Taheri et al. (2003). The data/information related to this problem is given below (Fig. 3).

Material Dimensions	:	350 WT Steel 100 x 300 x 5mm
Fracture toughness	:	50 MPa $\sqrt{}$m
Yield Strength	:	350 MPa

Stress ratio	:	0.1
Stress condition	:	Plane stress condition
Maximum stress	:	114 MPa
Minimum stress Crack growth Eqn.	:	11.4 MPa Paris
C m	:	1.02e-08 2.94
Initial crack length (a)	:	10 mm

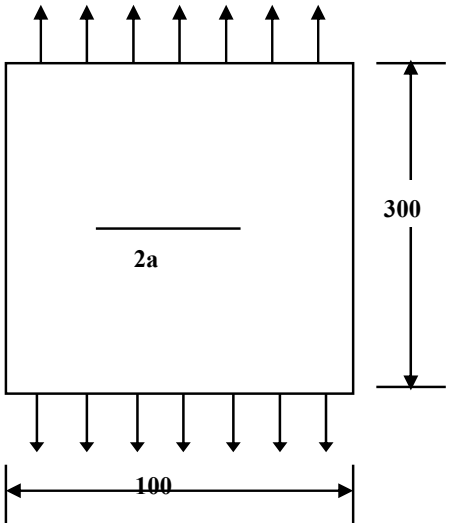

Figure 3: Plate with a centre crack

As a part of residual strength evaluation, remaining life has been predicted for the above problem and is given below. It can be observed that the predicted life is in good agreement with the corresponding experimental value available in the literature [Taheri et al.(2003)]. Fig. 4 shows the plot of crack length vs remaining life.

Present study = 138750 Cycles
Literature (Experimental) = 156000 Cycles
% difference = 11.05

Fig. 5 shows the plot of crack length vs residual strength predicted by using plastic collapse condition (yield condition), fracture toughness criterion and remaining life approach. It can be observed from Fig. 5 that the residual strength values predicted using remaining life approach are lower compared to those predicted by using other two approaches.

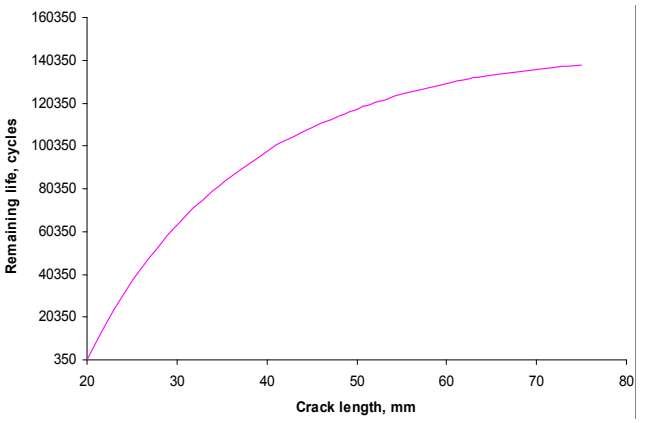

Figure 4: Crack length vs remaining life

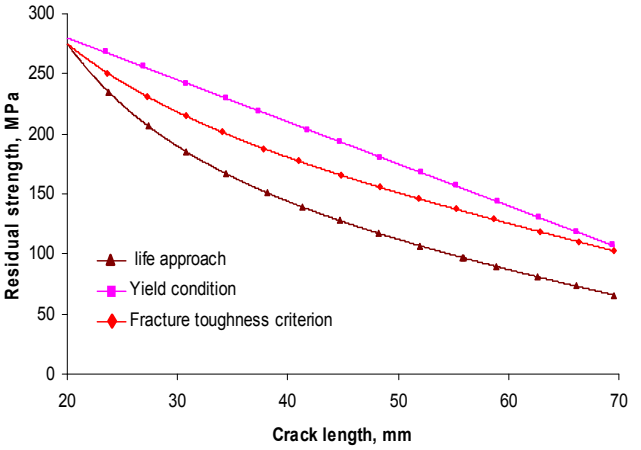

Figure 5: Crack length vs. residual strength

Fig. 6 shows the plot of remaining life vs. residual strength. This plot will be useful for the interpretation of residual strength with the known loading cycles.

5.2 CT-Specimen - 2024-T3 Al alloy

This example was studied by Stephens et al. (1976). The data/information related to this problem are given below (Fig. 7).

Material : 2024-T3 Al alloy

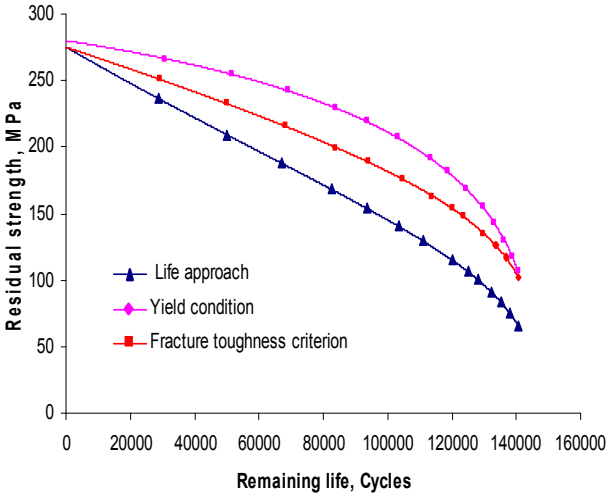

Figure 6: Remaining life vs. residual strength

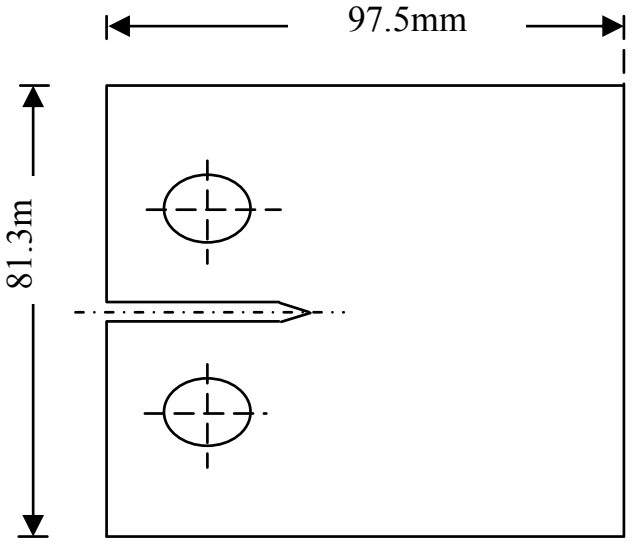

Figure 7: CT-Specimen

Plate dimensions	:	97.5 x 81.3mm
Thickness	:	9.15 mm
Fracture toughness	:	70.6 MPa $\sqrt{m}$

Yield Strength	:	355 MPa
Stress ratio	:	0.0
Stress condition at crack tip	:	Plane stress
Maximum stress (σ_{max})	:	103.99 MPa
Crack growth equation	:	Paris
C	:	0.199e-11
m	:	3.282
Initial crack length	:	25.4 mm

Fig. 8 shows the plot of crack length vs residual strength predicted using plastic collapse condition (yield condition), fracture toughness criterion and remaining life approach. It can be observed from Fig. 8 that the residual strength values predicted using remaining life approach are lower compared to those predicted by using other two approaches.

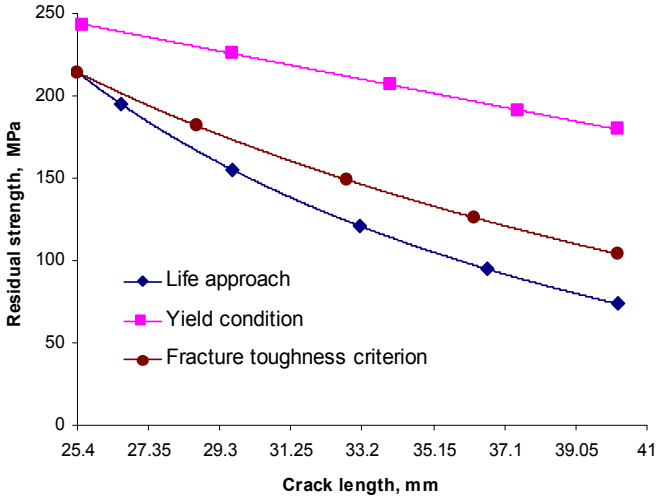

Figure 8: Crack length vs. residual strength

5.3 Stiffened plate with centre crack - 2024-T3 Al alloy

Another example problem, stiffened plate with a center crack has been studied for remaining life and residual strength evaluation (Fig. 9). This problem was studied by Dawicke (1997). The data/information related to this problem are given below.

Concentric and eccentric stiffening cases have been considered for remaining life and residual strength evaluation.

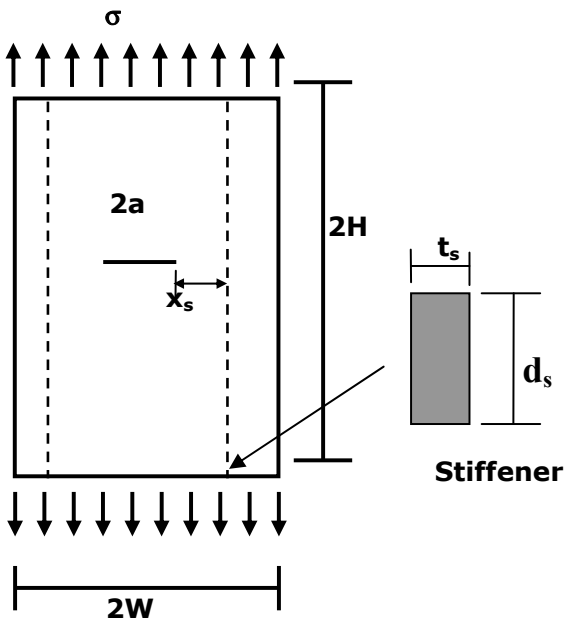

Figure 9: Stiffened plate with centre crack

Material	:	2024-T3 Al alloy
Plate dimensions	:	76.2 x 127 mm
Thickness	:	2.286 mm
Fracture toughness	:	50.54 MPa $\sqrt{}$m
Yield Strength	:	665.38 MPa
Stress ratio	:	0.02
Stress condition at crack tip	:	Plane stress
Maximum stress (σ_{max})	:	68.94 MPa
Crack growth equation	:	Paris
C	:	0.829e-8
m	:	2.284
Initial crack length	:	25.4 mm

Remaining life has been predicted without stiffener and observed that it is in good agreement with the corresponding value available in the literature.

Table 1: Remaining life for a plate with concentric stiffener

Stiffener area (mm^2)	Predicted remaining life when stiffener at X_s=6.35 mm	% diff. compared to unstiffened plate	Predicted remaining life when stiffener at edges	% diff. compared to unstiffened plate
unstiffened	28733	--	28733	--
16	2.4029×10^5	736.28	48434	68.56
20	2.6928×10^5	837.18	54190	88.59
24	2.9913×10^5	941.07	60565	110.79
28	3.2976×10^5	1047.67	68087	136.96
32	3.6104×10^5	1156.53	75954	164.34
36	3.928×10^5	1267.07	83135	189.34

Present study = 28733 cycles
Literature (Exptl.) = 30719 cycles
% difference = 6.91

5.3.1 Concentric stiffener case

In the case of concentric stiffener, remaining life and residual strength have been predicted for the stiffener located at x_s = 6.35 mm and at the edges. Table 1 shows the predicted remaining life for different stiffener sizes and positions under constant amplitude loading (CAL). Table 1 also shows the comparison of predicted remaining life for different stiffener sizes with the corresponding values of unstiffened case. Fig. 10 shows the variation of predicted remaining life under CAL for different stiffener sizes including the unstiffened case. From Table 1 and Fig. 10, it can be observed that the predicted life of stiffened panel under CAL increases with increase of stiffener area and is about 1267% higher for stiffener area of $36mm^2$ compared to the respective unstiffened case. It can also be observed that the predicted life is significantly higher for the stiffener located at x_s = 6.35 mm compared to the case of stiffener located at the edges.

Fig. 11 shows the predicted residual strength using remaining life approach for the stiffener areas of 16, 20, 24, 28, 32 and 36 mm^2 and unstiffened case. Stiffener is positioned at edges. From Fig. 11, it can be observed that, the predicted residual strength increases with increase of stiffener area. The predicted residual strength is 20.71 % and 45.11 % higher for the stiffener areas 16 and 36 mm^2 respectively

compared to unstiffened case. Fig. 12 shows the predicted residual strength using remaining life approach for the stiffener areas of 16, 20, 24, 28, 32 and 36 mm^2 and unstiffened case. Stiffener is positioned at 6.35 mm from crack tip. From Fig. 12, it can be observed that the predicted residual strength increases significantly with increase of stiffener area compared to unstiffened case. The predicted residual strength is 128.57 % and 201.48 % higher for the stiffener cases with area of 16 and 36 mm^2 respectively compared to unstiffened case. From Fig. 12, it can also be observed that the difference in the predicted residual strength for the stiffener case with area of 16 and 36 mm^2 reduces gradually with increase in crack length. From Figs. 11 and 12, it can be observed that the percentage increase in the predicted residual strength when the stiffener is placed at 6.35 mm is 89.36%, 95.92 %, 100.41%, 104.04%, 106.81% and 108.94% for the stiffener areas of 16, 20, 24, 28, 32 and 36 mm^2 respectively compared to that of the stiffener placed at the edges and for the same stiffener areas. Further, it can be observed from Figs. 11 and 12 that in the case of stiffener at edges the rate of decrease in residual strength w. r. t crack length is uniform for all the stiffness sizes, whereas for the case of stiffener at 6.35mm, the rate of decrease is gradually varying for different stiffener sizes. Polynomial curve fitting has been carried out using MATLAB software to get a best fit for each of the curves as shown in Figs. 11 and 12. The best fit equations for each of these curve obtained using the software have been given in eqns. (24) to (26). The error norm obtained for each of these best fit equations is also indicated. These equations will be useful for designers for prediction of residual strength of stiffened panels.

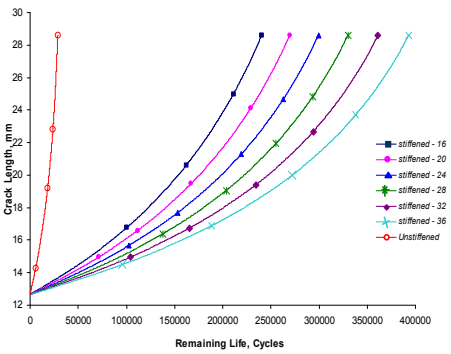

Figure 10: Remaining life for different stiffener sizes

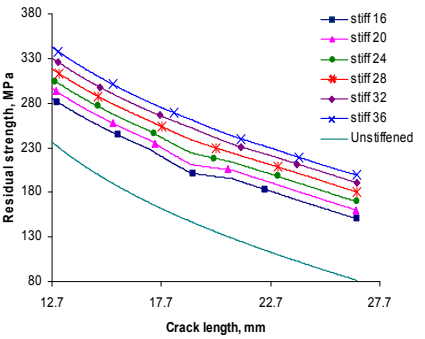

Figure 11: Half crack length vs. residual strength (Stiffener at edges)

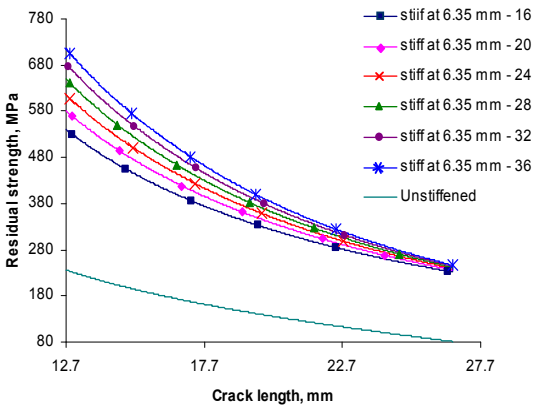

Figure 12: Half crack length vs residual strength

unstiffened case

$$\sigma_c = -0.023241a^3 + 1.7329a^2 - 51.131a + 652.74 \text{ (Error norm 5.562)} \quad (24)$$

Stiffener position at edges:

16mm^2

$$\sigma_c = -0.0052843a^4 + 0.38311a^3 - 9.7823a^2 + 92.819a + 36.091 \text{ (Error norm 5.125)} \quad (25a)$$

20mm^2

$$\sigma_c = -0.0056399a^4 + 0.41015a^3 - 10.523a^2 + 101.32a + 12.596 \text{ (Error norm 4.981)} \quad (25b)$$

24mm^2

$$\sigma_c = -0.0039142a^4 + 0.27907a^3 - 6.8863a^2 + 57.628a + 215.19 \text{ (Error norm 5.012)} \quad (25c)$$

28mm^2

$$\sigma_c = -0.0017628a^4 + 0.11562a^3 - 2.3511a^2 + 3.1853a + 465.47 \text{ (Error norm 4.967)} \quad (25d)$$

32mm^2

$$\sigma_c = 0.000512a^4 - 0.0190a^3 + 1.422a^2 - 42.803a + 683.16 \text{ (Error norm 4.892)} \quad (25e)$$

36mm^2

$$\sigma_c = 0.000478a^4 - 0.0578a^3 + 2.5977a^2 - 58.948a + 777.98 \text{ (Error norm 5.001)} \quad (25f)$$

Stiffener position at 6.35mm:

16mm^2

$$\sigma_c = -0.002888a^4 - 0.28428a^3 + 11.032a^2 - 211.19a + 1949.1 \text{ (Error norm 3.385)} \quad (26a)$$

20mm^2

$$\sigma_c = -0.0030306a^4 + 0.30054a^3 + 11.788a^2 - 228.74a + 2120.2 \text{ (Error norm 4.3094)} \quad (26b)$$

24mm^2

$$\sigma_c = -0.0031173a^4 - 0.31156a^3 + 12.354a^2 - 242.9a + 2263.8 \text{ (Error norm 5.3158)} \quad (26c)$$

28mm^2

$$\sigma_c = 0.0031683a^4 - 0.31961a^3 + 12.832a^2 - 255.97a + 2401.8 \text{ (Error norm 5.021)} \quad (26d)$$

32mm^2

$$\sigma_c = 0.003182a^4 - 0.32457a^3 + 13.22a^2 - 267.89a + 2533.9 \text{ (Error norm 5.210)} \quad (26e)$$

36mm^2

$$\sigma_c = -0.00049767a^5 + 0.052141a^4 - 2.2278a^3 + 49.878a^2 - 621.07a + 3929.5 \text{ (Error norm 5.7514)} \quad (26f)$$

where, σ_c is the residual strength and 'a' is half crack length.

5.3.2 Eccentric stiffener case

In this case, remaining life has been predicted for the stiffener position at x_s = 6.35 mm. Table 2 shows the predicted remaining life for different stiffener moments of inertia (MIs). Fig. 13 shows the variation of predicted remaining life for different stiffener MIs including the unstiffened case. From Fig. 13, it can be observed that the predicted life of stiffened panel increases with increase of stiffener MI and is about 379% higher for stiffener MI of 333 mm^4 compared to the respective unstiffened case.

Table 2: Remaining life for plate with a centre crack (eccentric stiffener)

Stiffener area (mm^4)	Remaining Life	% diff. compared to unstiffened plate
unstiffened	28733	–
0.5	1.3099 x 10^5	355.88
2.99	1.1845 x 10^5	312.24
10.66	1.217 x 10^5	323.55
23.04	1.2257 x 10^5	326.58
74.09	1.2903 x 10^5	349.06
149.38	1.3309 x 10^5	363.19
332.98	1.3773 x 10^5	379.34

Fig. 14 shows the predicted residual strength using remaining life approach for the stiffener MI of 0.5, 3, 10.66, 23.04, 74.09 and 149.38 mm^4 and unstiffened case. For this case also, stiffener position is assumed to be 6.35 mm. From Fig. 14, it can be observed that the predicted residual strength is larger for all the stiffener MIs compared to unstiffened case (62.9 to 69.12 %). Further it can be observed that the predicted residual strength increases with the increase of stiffener size. But the increase in the predicted residual strength is marginal with the increase of MI. As observed for the case of concentric, the rate of decrease of residual strength w. r. t crack length is varying gradually for different stiffener sizes. Polynomial curve fitting has been carried out using MATLAB software to get a best fit for each of the curves as shown in Fig. 14. The best fit equations for each of these curves obtained using the software have been given in eqn. (27a) to (27f). The error norm obtained for each of these best fit equations is also indicated. These equations will be useful for designers for prediction of residual strength of stiffened panels.

M*I = 0.5mm^4

$$\sigma_c = -0.031482a^3 + 2.4898a^2 - 72.609a + 968.86 \text{ (Error norm 8.1152)} \qquad (27a)$$

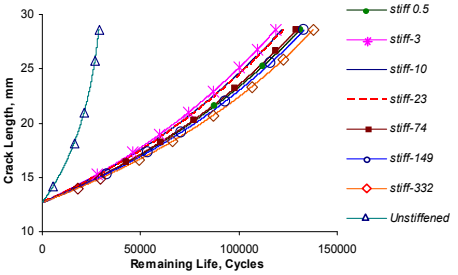

Figure 13: Remaining life for different stiffener MIs

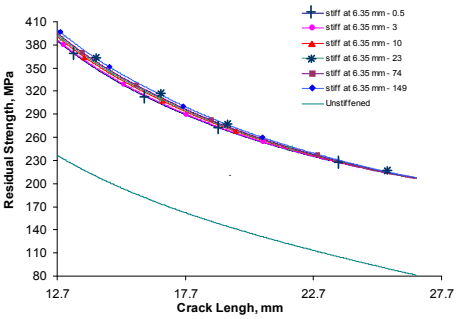

Figure 14: Residual strength for different stiffener MIs (eccentric case)

10.66mm^4

$$\sigma_c = -0.027218a^3 + 2.2297a^2 - 67.901a + 947.52 \text{ (Error norm 8.2272)} \quad (27b)$$

2.99mm^4

$$\sigma_c = -0.030147a^3 + 2.4075a^2 - 71.077a + 961.23 \text{ (Error norm 8.0787)} \quad (27c)$$

23.09mm^4

$$\sigma_c = -0.026491a^3 + 2.1881a^2 - 67.292a + 947.3 \text{ (Error norm 8.3441)} \quad (27d)$$

74.09mm^4

$$\sigma_c = -0.025943a^3 + 2.1577a^2 - 66.898a + 948.25 \text{ (Error norm 8.4584)} \quad (27e)$$

149.38mm^4

$$\sigma_c = -0.024954a^3 + 2.1049a^2 - 66.318a + 952.11 \text{ (Error norm 8.7225)} \quad (27f)$$

6 Summary and Concluding Remarks

To meet one of the requirements of damage tolerant evaluation, fracture mechanics based methodologies have been developed for residual strength evaluation of metallic structural components under fatigue loading. For reliable residual strength evaluation, the fracture parameter, namely, SIF is to be estimated accurately. SIF computation in the case of stiffened panels has been carried out by using the parametric equations based on NI-MVCCI technique. Procedure for remaining life

prediction is outlined. Various methods for residual strength evaluation, namely, plastic collapse condition, fracture toughness criterion and remaining life approach have been explained.

Numerical studies have been conducted on plate with centre crack and CT-specimen and observed that the predicted residual strength using remaining life approach is lower compared to those predicted by using other two approaches. Hence, it can be concluded that the residual strength predicted using remaining life approach will govern the design of structural components under fatigue loading.

Further, studies have also been conducted on stiffened panel with centre crack subjected to tension loading. Concentric and eccentric stiffener cases have been considered in the studies. Remaining life approach has been used for residual strength evaluation. From the studies, it is observed that the predicted residual strength increases with the increase of stiffener size in the case of concentric as well as eccentric case when compared to unstiffened case. It is further observed that in the case of stiffener at edges the rate of decrease in residual strength w. r. t crack length is uniform for all stiffener sizes, whereas for case of intermediate stiffener, the rate varies gradually for different stiffener sizes. Expressions for residual strength have been proposed considering various stiffener sizes, stiffener position and type of stiffener, which will be useful for designers to design the structural components/structures against fatigue and fracture.

Acknowledgement: We acknowledge with thanks the valuable technical suggestions and support provided by our colleagues Mr J. Rajasankar, Assistant Director and Ms. Smitha Gopinath, Scientist for useful technical discussions during the course of this investigation. This paper is being published with the permission of the Director, SERC, Chennai, India.

References

Alibadi, M.H. Wen, P.H. Salgado, N. (2002): Boundary element analysis for damage tolerance assessment of aircracft panels, *International Journal of Compuer Applications in Technology,* vol. 15(4-5), pp. 147-159.

Brussat, T.R., Kathiresan, K., Rudd, J.L. (1986): Damage tolerance assessment of aircraft attachment lugs, *Engg. Fract. Mech.*, vol. 23 (6) pp. 1067-1084.

Cali, C., Citarella. R. (2004): Residual strength assessment for a butt-joint in MSD condition, *Advances in Engineering Software*, vol. 35, pp. 373–382.

David Broek (1989): The practical use Fracture Mechanics, Kluwer Academic Publishers.

Dawicke, D.S.C. (1997): Overload and underload effects on the fatigue crack

growth behaviour of the 2024-T3 Aluminum Alloy, NASA Contractors Report 201668.

Irwin, G.R. (1957): Analysis of stress and strain near the end of a crack traversing a plate, *Jl. Applied Mechanics, ASME*, vol. 24, pp. 361-364.

Murakami, Y. (1988): *Stress intensity factors handbook*, Pergamon Press, Oxford.

Nathan, L. Post, John Bausano, Scott, w. case and John, J. Lesko (2006): Modelling the remaining strength of structural composite materials subjected to fatigue, *Int. Jl. Fatigue*, vol. 28, pp. 1100-1108.

Nathan, L. Post, J. Cain, K.J. McDonald, S.W. case and Lesko, J. J. (2008): Residual strength prediction of composite materials; Random spectrum loading, *Engg. Fract. Mech*. Vol. 75(9) pp. 2707-2724.

Palani, G.S. (2004): Numerically integrated MVCCI technique for fracture analysis of plates and stiffened panels, PhD thesis, Indian Institute of Science, Bangalore,

Palani, G.S., Nagesh R. Iyer and Dattaguru, B. (2005): Fracture analysis of cracked stiffened panels under combined tensile, bending and shear loads, *AIAA Jl*, vol. 43, pp. 2039-2045.

Paris, P.C., Erdogan, F. (1963): A critical analysis of crack propagation laws, *Jl. Basic Engg*., vol. 85, pp. 528-534.

Rooke, D.P., Cartwright, D.J. (1976): Compendium of stress intensity factors, Her Majesty's Stationary Office, London.

Stephens, R.I., Chen Hom, B.W. (1976): Fatigue crack growth with negative stress ratio following single overloads in 2024-T3 and 7075-T6 aluminum alloys, *ASTM STP* vol. 595, pp. 27-40.

Swift, T. (1984): Fracture analysis of stiffened structure, *Damage Tolerance of Metallic Structures, Analysis Methods and Application*, ASTM STP842, pp. 69-107.

Taheri, F., Trask, D., Pegg, N. (2003): Experimental and analytical investigation of fatigue characteristics of 350WT steel under constant and variable amplitude loadings, *Marine Structures*, vol. 16, pp. 69-91.

Toor, M. Pir, Double Dagger (1987): On damage tolerance design of fuselage structure (circumferential cracks), *Engg. Fract. Mech.*, vol. 26(5), pp. 771-782.

Toor M. Pir, Double Dagger (1986): On damage tolerance design of fuselage structure (longitudinal cracks), *Engg. Fract. Mech.*, vol. 24(6) pp. 915-927.

Toor, M. Pir (1973): A review of some damage tolerance design approaches for aircraft structures, *Engg. Fract. Mech.*, vol. **5**(4) pp. 837-876.

Wang John, T., Clarence, C. Poe, Damodar, R. Ambur and David W. Sleight

(2006): Residual strength prediction of damaged composite fuselage panel with R-curve method, *Composites Science and Technology*, vol. 66, pp. 2557–2565.

Wen, P. H. Alibadi, M.H., Young, A. (2002): Boundary element analysis of flat cracked panels with adhesively bonded patches, *Engg. Fract. Mech*, vol. 69, pp. 2129-2146.

Wood, A. Howard (1975): Application of fracture mechanics to aircraft structural safety, *Engg. Fract. Mech*., vol. **7**(3), pp. 557-558.